

## The Earth's Magnetosphere Features During the Quiet 2009–2010 Epoch

W. O. Barinova, V. V. Kalegaev, I. N. Myagkova, D. A. Parunakian, I. Rubinstein,  
M. O. Riazantseva

Skobeltsyn Institute of Nuclear Physics, Moscow State University, Moscow, Russian Federation

**Abstract.** We study the global magnetospheric structure and its dynamics during extremely quiet geomagnetic conditions in the 2009-2010 epoch using satellite measurements. We determine the mean position of the outer radiation belt (ORB) boundaries at the Earth surface using regular measurements of  $E > 200$  keV electron fluxes onboard Coronas-Photon since March till November 2009 and  $E > 100$  keV electron fluxes onboard Meteor-M #1 since November 2009 till May 2010. These low altitude polar satellites crossed the external boundaries of ORB in both hemispheres approximately every 1.5 hrs. It was obtained that the high-latitude ORB boundary is controlled by both geomagnetic (internal) and magnetospheric magnetic fields. The extremely quiet conditions allowed us to separate the effects induced by internal and external factors. It has been found that at the ionospheric level the high-latitude boundary of ORB rotates with the Earth but slightly shifts to the night side due to large-scale magnetospheric currents. Variation of ORB boundaries have been determined to depend on UT (universal time).

### Introduction

Monitoring of the near-Earth environment is important for ensuring spacecraft safety and preventing electronic equipment malfunctions caused by increases of relativistic electron fluxes in the outer radiation belt, especially during magnetic storms [1]. Experiments probing the dynamics of outer radiation belt electron fluxes have been conducted almost since the radiation belt was discovered. The motion of charged particles of radiation belts is determined by a specific configuration of the magnetosphere. Changes of the magnetospheric magnetic field structure under the solar wind and interplanetary magnetic field (IMF) driving reveal themselves in variations of fluxes of charged particles. It is well known that the outer radiation belt particle fluxes abruptly change during geomagnetic storms [1], which are induced either by arrival of coronal mass ejections [2-3] or high-speed fluxes of the solar wind [4]. The size of the trapped radiation region is also very sensitive to the solar wind speed and geomagnetic activity [1]. During the magnetic storm main phase of CME- and CIR-driven storms when the  $Dst$  index reaches the minimum, the locations of the outer boundary move to  $L=4$  and  $L=5.5$ , respectively [5]. Some peculiarities of outer radiation belt dynamics (position of maximum fluxes of relativistic electrons, location of rapid enhancements of the electron fluxes) were studied in [6-8].

Radiation conditions in the quiet magnetosphere are also controlled by fluxes of high-energy electrons in the outer radiation belt. In the quiet magnetosphere when the solar wind influence is negligible, the high-latitude outer radiation belt boundary location is relatively stable and reflects mainly the global magnetic field structure. Dynamical changes of the magnetic field are due to a rotation of the Earth internal magnetic field relatively to global magnetospheric current systems producing the external magnetospheric field.

Dynamics of the outer radiation belt high-latitude boundary and variations of its position can be observed onboard LEO (Low Earth Orbit) satellites. Using measurements during the extremely quiet epoch of 2009-spring 2010, we are able to identify how its geometry depends on the quiet magnetospheric magnetic field without an influence of external factors. The results of measurements onboard the Coronas-Photon orbital solar observatory and Meteor-M#1 spacecraft have been used in analysis of the dynamics of the quiet outer radiation belt high-latitude boundary.

### Experiments

Since both the Coronas-Photon solar observatory (the third spacecraft in the Coronas series) and the Meteor-M#1 satellite had circular polar orbits (Coronas-Photon: 550 km altitude, 82.5 deg.

inclination; Meteor-M#1: 832 km altitude, 101.3 deg. inclination), it was possible to use their onboard instruments to monitor the Earth outer radiation belt at low altitudes.

Built in SINP MSU (Skobeltsyn Institute of Nuclear Physics, Moscow State University), the Electron-M-Pesca instrument consisted of two parallel four-element semiconductor telescopes designed to detect protons (4–80 MeV), electrons (0.2–3 MeV), alpha particles (5–24 MeV/nucl), particles of CNO (Carbon, Nitrogen and Oxygen nuclei) group (6–15 MeV/nucl) in near-Earth space. The instrument registered fluxes of particles—up to  $5 \cdot 10^7 \text{ cm}^{-2} \cdot \text{s}^{-1} \cdot \text{ster}^{-1}$ . A detailed description of Electron-M-Pesca design and operating principles can be found in [9].

The MSGI instrument installed onboard the Meteor-M#1 spacecraft consists of a number of semiconductor and scintillation detectors and is used to measurements of energetic particle fluxes (0.1–13 MeV electrons and 1–260 MeV protons) [10].

### Interplanetary space conditions during October 2009 - May 2010

The solar and Earth magnetosphere conditions during October 2009-May 2010 have been extremely quiet. We can use this period to better understand, what quiet magnetosphere is. Let's look at the results of calculating the distribution and average values of the solar wind and IMF. Figure 1 shows distributions of the solar wind (SW) and IMF parameters measured during this period.

Z-component of the IMF vector in the solar-magnetospheric coordinate system (GSM),  $b_z$  is one of the most geoeffective factor influencing the magnetosphere. In 2009–2010,  $b_z$  (Figure 1a) was too low in absolutely value ( $\langle |b_z| \rangle = 1.35 \text{ nT}$ ) and even positive, while  $\langle b_z \rangle = +0.118 \text{ nT}$  (Figure 1b).

We can see that while the solar wind velocity (Figure 1c) average value is close to usual ( $\langle v \rangle = 358.4 \text{ km/sec}$ ), the plasma density (Figure 1d) is twice lower than usually measured during quiet days in the standard epoch ( $\langle n \rangle = 3.16 \text{ cm}^{-3}$ ), so the SW pressure (Figure 1e) is also too low ( $\langle \text{PSW} \rangle = 0.75 \text{ nPa}$ ). The IMF is also smaller than standard reference values and it means that the solar wind should be less geoeffective.

### Outer radiation belt high latitude boundary position in extremely quiet geomagnetic conditions

To analyze the dynamics of the outer radiation belt high-latitude boundary position in extremely quiet geomagnetic conditions, we have developed a numeric method that allows to automatically determine ionospheric coordinates of the outer radiation belt high-latitude boundary detected along the spacecraft trajectory. Using statistic analysis, we found two fastest and longest increase and decrease of charged particle count rates nearest to the magnetic pole in each time the satellite crossed the polar region. We detect time and coordinates of the end of decrease and the beginning of increase and saved all points into database. Then, we plot all of them in the polar coordinate system.

During November 2009, both Coronas-Photon and Meteor-M#1 satellites provided simultaneous observations. Figure 2 shows the polar diagram with outer radiation belt high-latitude boundary crossings. The light squares denote the geographic coordinates of crossings obtained from Coronas-Photon measurements of  $>200 \text{ keV}$  electron fluxes in the northern hemisphere mapped to 100 km altitude, while the black squares denote similar data based on Meteor-M #1 measurements of  $>100 \text{ keV}$  electrons.

### Energy dependent dynamics of ORB high-latitude boundary

As it seen in Figure 2, the mean position of the boundary at these altitudes has an ellipse shape. The position of the ellipse at the ionospheric level is determined by the specific features of the Earth's magnetic field, namely the position of the North magnetic pole and the intensity of its non-dipole harmonics. Data points of measurements on the satellites fluctuate by approximately 5 degrees indicating the influence of the magnetospheric magnetic field dependent on UT. We observe a good conformity of the shape of the trapped radiation boundary built based on the measurements of the two satellites. Discrepancies between the positions of the high-latitude boundary obtained from different spacecraft data are due to the difference in measured particle energies: the boundary of lower energy particles from Meteor-M#1 measurements ( $>100 \text{ keV}$ ) is located closer to the pole than the boundary of higher energy particles measured by Coronas-Photon ( $>200 \text{ keV}$ ). As it seen in Figure 2, the shift is approximately 2 degrees of latitude.

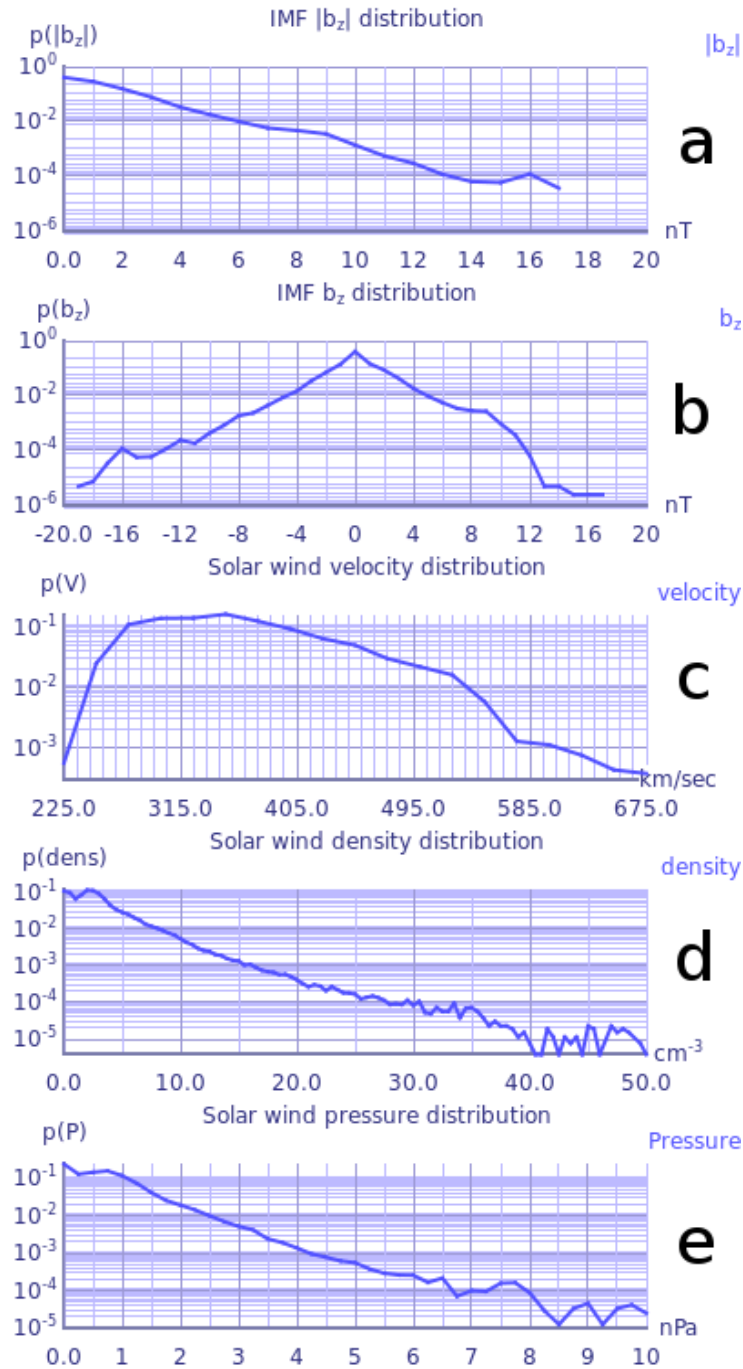


**Figure 1.** Distributions of the solar wind parameters during the quiet 2009–2010 epoch: **(a)** IMF  $|b_z|$  distribution, **(b)** IMF  $b_z$  distribution, **(c)** SW velocity distribution, **(d)** SW density distribution, **(e)** SW pressure distribution.

### UT dependent dynamics of ORB high-latitude boundary

Radiation belts rotate with the Earth. For the same local time high-latitude outer radiation belt boundary will be located at different latitudes depending on UT. This is the primary effect of rotating geomagnetic field structure, non-symmetrical relatively to the Earth's axis and non-dipolar one. The second order effect is the magnetospheric current influence. The noon-midnight magnetic field asymmetry provides the shift of all magnetospheric domains especially significant in the polar regions. We can estimate such shift of high-latitude boundary of the trapped particles obtained from Meteor-M #1 and Coronas-Photon measurements. Fortunately, during 2009–2010, the solar activity was extremely quiet and didn't contaminate the effect of magnetospheric currents.

We can estimate this effect from the Coronas-Photon database of ORB high-latitude boundary crossings collected for different UT through 2009. It means that we study variations of the ORB boundary in dependence on the angle between the Greenwich meridian and Sun-Earth line. Figure 3 demonstrates two cases together: the data points obtained from satellite crossings of the high-latitude ORB boundary between 15–21 UT (mean value is 18 UT, dark points) and between 3–9 UT (mean value is 6 UT, light points).

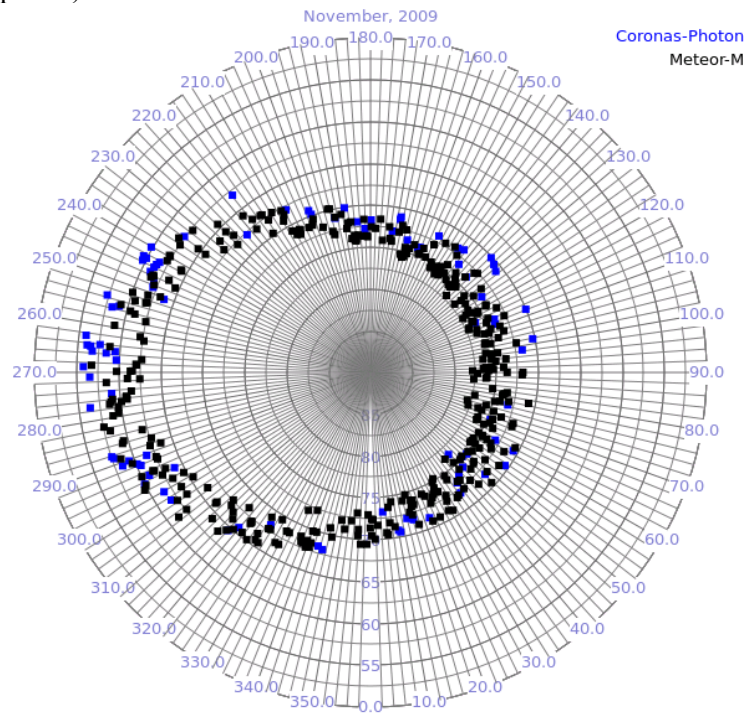


**Figure 2.** Distribution of high latitude outer radiation belt boundary crossings obtained in the Northern hemisphere from Coronas-Photon and Meteor-M #1 measurements during November 2009 in geographical polar coordinates.

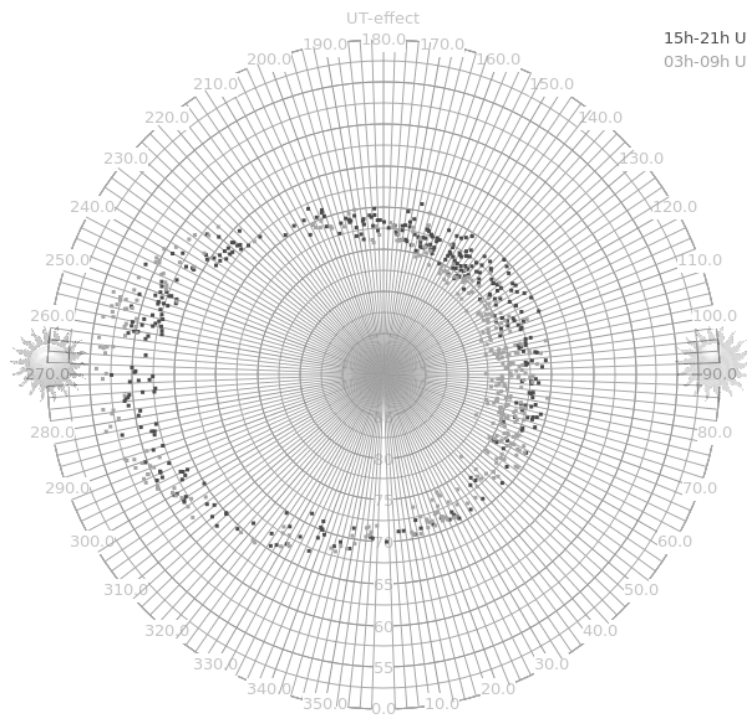


**Figure 3.** ORB external boundary crossings by CPh around 6 and 18 UT.

At 6 UT, when the Sun is approximately above 90 degree meridian the high-latitude boundary crossings shift anti-sunward relatively to boundary crossings obtained near 18 UT when the Sun was approximately above 270 degree meridian.

Two data arrays shift to the midnight each and one can see about the 3 deg difference between average locations of them. We suggested that the ellipse keeps its orientation relatively to the Earth surface and rotates together with the Earth. We have analyzed different pictures for the whole day and we have concluded that the average statistical ellipse only shifts to midnight and the shift size is about 1.5 degree from the average position. The centre of the average ellipse looks like located in the magnetic pole.

## Conclusions

Comparison of the outer radiation belt boundary position estimated using measurements conducted onboard the Coronas-Photon and Meteor-M#1 during November 2009 indicates that when taking into account the difference in registered particle energies, the data produced in these two experiments are in a good accordance.

The mean position of the boundary that has an ellipse shape at the ionospheric level was mostly influenced by the geomagnetic field generated by currents in the Earth's core. We also studied how the boundary position changes depending on the particle energy. It was established that the boundary is located closer to the magnetic pole by approximately 2 degrees for lower energy particles (Meteor-M#1, >100 keV) than for higher energy particles (Coronas-Photon, > 200 keV).

During the extremely quiet solar wind conditions in 2009–2010 (the low SW density and low IMF), the outer radiation belt high-latitude boundary location depends mainly on the internal Earth's magnetic field and on quiet magnetospheric currents. Its dynamics is due to the Earth's rotation and continuous influence of the magnetospheric currents responsible for the magnetospheric noon-midnight asymmetry. The noon-midnight shift of the ORB high-latitude boundary due to magnetospheric currents is about 1.5 degree.

**Acknowledgements.** This work has been sponsored by the Russian Federation President's grant "K 1579-2010.2" and RFBR grant 09-05-00978. All data are collected on site of the Space Monitoring Data Center of SINP/MSU [smdc.sinp.msu.ru](http://smdc.sinp.msu.ru) and updated daily.

## References

- [1] Kuznetsov S. N., Tverskaya L. V., Space Model, 1, Physical space conditions, Chapt. 3.4 Radiation Belts (edited by Panasyuk M.I.), Moscow, MSU, Knizny dom, pp. 518–546, 2007.
- [2] Panasyuk M. I., Kuznetsov S. N., Lazutin L. L., et al., Magnetic storms in 2003, October, Space Research 42, N 5, 509–554, 2004.
- [3] Gopalswamy, N., Coronal Mass Ejections of Solar Cycle 23, Astron. Astrophys. 27, 243-254, 2006.
- [4] Li X., D. N. Baker, M. Temerin, G. D. Reeves, R. Friedel, and C. Shen, Energetic electrons, 50 keV-6 MeV, at geosynchronous orbit: their responses to solar wind variations, Space Weather 3, S04001, doi:10.1029/2004SW000105, 2005.
- [5] Yuan C J., Zong Q G., Dynamic variations of the outer radiation belt during magnetic storms for 1.5-6.0 MeV electrons, Sci. China Tech. Sci. 54, 431–440, DOI: 10.1007/s11431-010-4269-9, 2011.
- [6] Myagkova I. M., Riazantseva M. O., Antonova E. E., et al., Enhancements of fluxes of precipitating energetic electrons on the boundary of the outer radiation belt of the earth and position of the auroral oval boundaries, Cosmic Res. 48, 165–173, DOI: 10.1134/S0010952510020061, 2010.
- [7] Tverskaya L. V., Balashov S. V., Vedenkin N. N., et al., Solar Proton Increases and Dynamics of the Electron Outer Radiation Belt during Solar Events in December 2006, Geomag. and Aeronom. 48, 719–726, DOI: 10.1134/S0016793208060042, 2008.
- [8] Tverskaya L.V.; Ginzburg E.A.; Ivanova T.A.; et al., Peculiarities of the outer radiation belt dynamics during the strong magnetic storm of May 15, 2005, Geomag. and Aeronom. 47, 696–703, DOI: 10.1134/S0016793207060023, 2007.
- [9] Denisov Yu. I., Kalegaev V. V., Myagkova I. N., Panasyuk M. I., Astronomichesky vestnik, 3, 15–24, 2011.
- [10] [http://smdc.sinp.msu.ru/index.py?nav=meteor\\_m&switchdiv=Overview](http://smdc.sinp.msu.ru/index.py?nav=meteor_m&switchdiv=Overview)